

on virtual simulation platforms that can be used to merge digital images (MRI pre, MRI post, 2D tomographies, 3D tomographies). Once the virtual surgical planning had been completed, navigation-guided surgery can be used to achieve tumor-free margins with an accuracy of millimeters.

As the tumor had been resected in a previous procedure, we had to decide the anatomical limits for oncological resection with tumor-free margins. We decided to use virtual surgical planning based on a magnetic resonance image obtained prior to the initial surgery, which showed the soft-tissue lesion in contact with the 8th, 9th, and 10th ribs (Fig. 1A). The lesion was reconstructed virtually in a new CT scan performed on the same day of surgery (Fig. 1B). Using the intraoperative navigation system, oncological resection of the chest wall *en bloc* with soft tissues was performed, and 3 rib sections were resected (Fig. 1C and D) and reconstructed with osteosynthesis material. The postoperative period was incident-free, and the patient was discharged on day 6 post-procedure.

Primary tumors of the chest wall are rare cancers that represent less than 5% of all thoracic tumors. The 3 most common subtypes are chondrosarcomas, liposarcomas, and fibrosarcomas. Surgical resection with adequate tumor-free margins is critical to achieve the best oncological outcome. Surgeons should have a broad knowledge of the principles and different methods of chest wall resection and reconstruction.<sup>1</sup>

The importance of computer-assisted surgery in providing support for both preoperative and intraoperative planning, especially in patients with oncological disease, has already been established in the literature.<sup>2</sup>

In chest wall tumors, intraoperative navigation is used to orient the surgeon in the 3-dimensional space and guide the surgery by matching the images acquired and processed before surgery with real anatomical landmarks.<sup>3</sup>

We report a situation which, to our knowledge, has not been previously described in the literature. Magnetic resonance images obtained before the initial surgery were merged with

images of a subsequent computed tomography in which the lesion was no longer present (per surgical history). Virtual reconstruction of the resected lesion allowed us to perform oncological surgery obtaining tumor-free margins in a previously operated patient.

## References

1. Shah AC, Komperda KW, Mavanur AA, Thorpe SW, Weiss KR, Goodman MA. Overall survival and tumor recurrence after surgical resection for primary malignant chest wall tumors: a single-center, single-surgeon experience [Internet]. *J Orthop Surg*. 2019. <http://dx.doi.org/10.1177/2309499019838296>, 2309499019838296.
2. Stella F, Dolci G, Dell'Amore A, Badiali G, De Matteis M, Asadi N, et al. Three-dimensional surgical simulation-guided navigation in thoracic surgery: a new approach to improve results in chest wall resection and reconstruction for malignant diseases. *Interact Cardiovasc Thorac Surg*. 2014;18:7–12.
3. Ritacco LE, Smith DE, Mancino AV, Farfalli GL, Aponte-Tinao LA, Milano FE. Accuracy of chest wall tumor resection guided by navigation: Experimental model. *Stud Health Technol Inform*. 2015;216:1026.

Soledad Belen Olivera Lopez,<sup>a</sup> Lucas Eduardo Ritacco,<sup>b</sup> Agustin Dietrich,<sup>c,\*</sup> Juan Alejandro Montagne,<sup>c</sup> David Eduardo Smith<sup>c</sup>

<sup>a</sup> Servicio de Cirugía General, Hospital Italiano de Buenos Aires, Buenos Aires, Argentina

<sup>b</sup> Unidad de Cirugía Asistida por Computadora, Hospital Italiano de Buenos Aires, Buenos Aires, Argentina

<sup>c</sup> Servicio de Cirugía Torácica y Trasplante Pulmonar, Hospital Italiano de Buenos Aires, Buenos Aires, Argentina

Corresponding author.

E-mail address: [agustin.dietrich@hospitalitaliano.org.ar](mailto:agustin.dietrich@hospitalitaliano.org.ar) (A. Dietrich).

Received 8 July 2019

Accepted 30 July 2019

<https://doi.org/10.1016/j.arbr.2019.07.009>

1579-2129/ © 2020 Published by Elsevier España, S.L.U. on behalf of SEPAR.

## Biophysically Preconditioning Mesenchymal Stem Cells Improves Treatment of Ventilator-Induced Lung Injury



### El acondicionamiento biofísico de las células madre mesenquimales mejora el tratamiento del daño pulmonar inducido por ventilación

Dear Editor:

Acute respiratory distress syndrome (ARDS) is still associated with high mortality despite the considerable efforts devoted to improving its treatment from the perspectives of basic science and clinical research. Cell therapy was proposed as a potential new tool for treating ARDS and the results obtained so far from preclinical research are encouraging.<sup>1</sup> Mesenchymal stem (stromal) cells (MSCs) are particularly interesting for this application, not because of their potential differentiation into lung cell phenotypes, but because of their ability to release agents (e.g., paracrine factors, microvesicles, mitochondria) with immunomodulatory, anti-inflammatory and antimicrobial effects.<sup>2–4</sup> The promising results obtained using MSCs in animal and *ex vivo* human lung ARDS models provided background to launch the first clinical trials which have recently finished or are still in progress.<sup>5,6</sup> However, determining the technical details (e.g. cell origin and preparation, administration procedure and dosage) to optimize

the potential therapeutic effects of MSCs in ARDS is still an open issue.<sup>1</sup>

Preconditioning MSCs before their application to patients could be relevant since it would pre-activate repair physiological pathways in these cells. It is known that modifying the microenvironment of MSCs modulates their paracrine signalling.<sup>7</sup> In particular, MSCs sense and actively respond to their biophysical microenvironment. For example, secretion of a wide range of cytokines is regulated by the stiffness of MSCs microenvironment<sup>8</sup> and stretching enhances angiogenic and anti-apoptotic capacities in these cells.<sup>9,10</sup> The fact that MSCs exhibit such responses to biophysical stimuli is particularly interesting for treating ARDS since cells in the target organ are placed on microenvironments with different stiffness<sup>11</sup> and undergo continuous mechanical stretching owing to ventilation. Therefore, we hypothesized that preconditioning MSCs by subjecting them to conditions realistically mimicking the biophysical microenvironment in the lung would improve their effectiveness in the treatment of ARDS. Here we describe a proof of concept test of this hypothesis. The study (approved by the Institutional Ethics Board) was carried out on a rat model (Sprague Dawley, male, 200–300 g) of ventilator-induced lung injury (VILI). Specifically, we biophysically preconditioned MSCs by culturing the cells on lung extracellular matrix (ECM) to expose them to realistic biochemical and stiffness substrate cues and by simultaneously subjecting MSCs to cyclical stretch simulating ventilation.

Lung-derived MSCs were obtained from Sprague Dawley rats<sup>12</sup> weighing 200–300 g and conventionally characterized by their cell surface markers (CD29, CD44H, CD45, CD11b/c and CD90) and differentiation capability (adipocytes, osteocytes and chondrocytes). Moreover, 70- $\mu$ m slices of lung ECM obtained by decellularizing rat lungs<sup>11</sup> were attached on the flexible membrane of computer-controlled polydimethylsiloxane (PDMS) chip specifically designed to subject cells to frequency- and amplitude-controlled dynamic stretch by applying cyclical positive pressure underneath the membrane.<sup>13</sup> Subsequently, MSCs were mechanically preconditioned by seeding them on the lung ECM slices and subjected to cyclic stretch mimicking lung ventilation (20% amplitude, 12 cycles/min) for 7 days. Additionally, non-preconditioned MSCs were cultured in parallel in conventional flasks.

Both MSCs with/without preconditioning were used to treat VILI induced in anesthetized, tracheostomized and paralyzed Sprague Dawley rats initially subjected to baseline ventilation (7 mL/kg, PEEP = 3 cmH<sub>2</sub>O, 70 cycles/min, 21% O<sub>2</sub>) and then subjected to injurious ventilation (35 cmH<sub>2</sub>O inspiratory pressure, zero PEEP) until achieving an increase of ~20% in respiratory elastance, which would induce a relatively mild VILI.<sup>14</sup> Injurious ventilation time was 103  $\pm$  18 min ( $m \pm$  SD), with no significant difference among groups ( $P = .665$ , One Way ANOVA). After this time point, baseline ventilation was resumed for 30 min and treatment with MSCs was applied by femoral venous injection. To this end, rats with VILI were randomly distributed into 3 treatment groups ( $N = 8$  each): vehicle, non-preconditioned MSCs and preconditioned MSCs ( $4 \times 10^6$  cells/kg in 500  $\mu$ L, in both cases). After treatment, the rats were kept under baseline ventilation for 4 h and then (end-point) elastance was measured, bronchoalveolar lavage fluid (BALF) was obtained from one lung for measuring total cell, neutrophil, protein and inflammatory cytokines (TNF- $\alpha$  and CXCL2) concentrations, and the other lung was excised for assessing oedema by its weight/dry ratio.<sup>15</sup> A group of control rats ( $N = 8$ ) was maintained under initial ventilation (no VILI, no treatment) for the same total time. MSCs engraftment in the lungs was assessed in additional VILI rats treated with fluorescently (PKH26) stained MSCs with/without ( $N = 6$  each) preconditioning.

After a ~20% increase in elastance, established by protocol, only preconditioned MSCs induced a significant recovery in elastance (Fig. 1A; paired  $t$ -test). In VILI, lung oedema increased by 16% and all the other 6 outcome variables augmented by more than 2-fold (Fig. 1B), reflecting typical increase in alveolar-capillary membrane permeability and inflammation. The statistical significance of the overall effect of VILI treatment with MSCs was assessed by conducting a rank-ANOVA to the sum of the 6 outcome variables after applying a normal standardization (Fig. 1B). The novel and relevant result of this study, which confirms our hypothesis, was that biophysically preconditioned MSCs were more effective than non-preconditioned MSCs in reducing VILI. In fact, while the effect of non-preconditioned MSCs was low, preconditioned MSCs achieved a significant recovery from VILI (Fig. 1B). This improvement in treatment was not associated with a significant difference in MSC engraftment into the lungs ( $P = .997$ ,  $t$ -test).

This is the first study providing support to the novel notion that biophysically preconditioning MSCs could optimize the therapy in ARDS. However, like any proof of concept test, our study has limitations since lung histology, gas exchange, systemic inflammation and repair mechanisms potentially involved (e.g. keratinocyte growth factor<sup>14</sup>) were not assessed. Notwithstanding, this work opens a considerable number of important questions. Among the more specific, whether the positive effects of biophysically preconditioned MSCs we observed would be reproduced in a more severe and long-term VILI model. More general questions include the comparison of the effects of preconditioning lung-derived vs bone

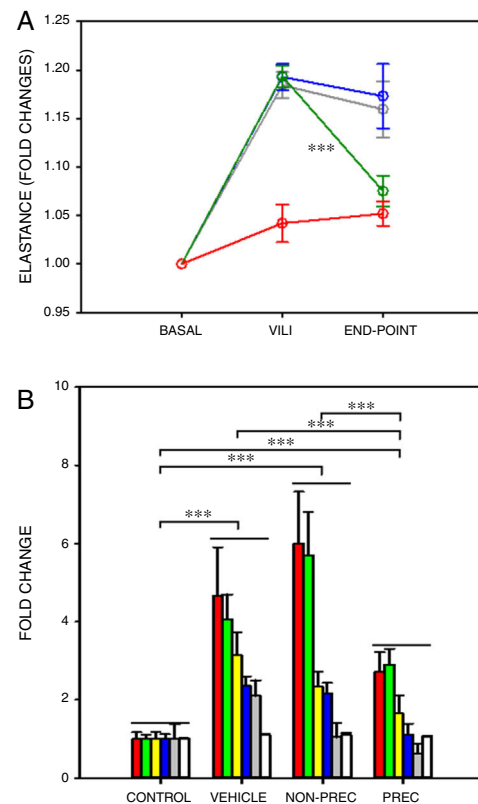


**Fig. 1.** Biophysically preconditioned MSCs reduced VILI. (A) Time course of respiratory elastance (relative to baseline value) in rats subjected to VILI and treated with: vehicle (no-MSCs) (grey), non-preconditioned MSCs (blue) and preconditioned MSCs (green). Red line corresponds to rats maintained with baseline ventilation (no VILI induction). \*\*\* Means  $P < .001$  comparing elastance measured after 30 min of injured ventilation (VILI) and after 4 h of treatment (END-POINT) with paired  $t$ -test. (B) Fold changes measured at the END-POINT in lung oedema (white) and bronchoalveolar lavage fluid concentrations of proteins (green), total cells (red), neutrophils (grey), TNF- $\alpha$  (blue) and CXCL2 (yellow), for control ventilation (CONTROL: no VILI induction) and treatment with: VEHICLE (no-MSCs), non-preconditioned (NON-PREC) MSCs and preconditioned (PREC) MSCs. Data are mean  $\pm$  SE. \*\*\* Means  $P < .001$  in a rank-ANOVA to the sum of these 6 variables after applying a normal standardization.

marrow-derived MSCs, or application of MSCs vs their supernatant, extracellular vesicles or mRNAs. It would also be important to test the effects of biophysically preconditioned MSCs on other experimental one-hit or two-hit models of intra- and extra-pulmonary ARDS (e.g. induced by LPS, bacterial lung infection, acid lavage, intra-abdominal or systemic sepsis).

In conclusion, we believe that this study opens an avenue for future research aimed at understanding the basic repair mechanisms activated in MSCs by physiometric stimuli, with the translational perspective towards the use of these cells as a tool to improve the treatment of lung injury.

## Funding

This work was supported in part by the Spanish Ministry of Economy and Competitiveness (SAF2017-85574-R, DPI2017-83721-P) and Generalitat de Catalunya (Programa CERCA). PNN was supported by National Counsel of Technological and Scientific Development from Brazil – CNPq (207258/2014-7).

## Acknowledgments

The authors wish to thank Dr. Ferran Torres, Medical Statistics Core Facility, Institut Investigacions Biomediques August Pi Sunyer, for his support in the statistical analysis of the data.

## References

- Laffey JG, Matthay MA. Fifty years of research in ARDS cell-based therapy for acute respiratory distress syndrome. Biology and potential therapeutic value. *Am J Respir Crit Care Med*. 2017;196:266–73.
- Park J, Kim S, Lim H, Liu A, Hu S, Lee J, et al. Therapeutic effects of human mesenchymal stem cell microvesicles in an ex vivo perfused human lung injured with severe *E. coli* pneumonia. *Thorax*. 2019;74:43–50.
- Rabani R, Volchuk A, Jerkic M, Ormisher L, Garces-Ramirez L, Canton J, et al. Mesenchymal stem cells enhance NOX2-dependent reactive oxygen species production and bacterial killing in macrophages during sepsis. *Eur Respir J*. 2018;51.
- Morrison TJ, Jackson MV, Cunningham EK, Kissenpfennig A, McAuley DF, O’Kane CM, et al. Mesenchymal stromal cells modulate macrophages in clinically relevant lung injury models by extracellular vesicle mitochondrial transfer. *Am J Respir Crit Care Med*. 2017;196:1275–86.
- Huppert LA, Liu KD, Matthay MA. Therapeutic potential of mesenchymal stromal cells in the treatment of ARDS. *Transfusion*. 2019;59(S1):869–75.
- Matthay MA, Calfee CS, Zhuo H, Thompson BT, Wilson JG, Levitt JE, et al. Treatment with allogeneic mesenchymal stromal cells for moderate to severe acute respiratory distress syndrome (START study): a randomised phase 2a safety trial. *Lancet Respir Med*. 2019;7:154–62.
- Kusuma GD, Carthew J, Lim R, Frith JE. Effect of the microenvironment on mesenchymal stem cell paracrine signaling: opportunities to engineer the therapeutic effect. *Stem Cells Dev*. 2017;26:617–31.
- Darnell M, O’Neil A, Mao A, Gu L, Rubin LL, Mooney DJ. Material microenvironmental properties couple to induce distinct transcriptional programs in mammalian stem cells. *Proc Natl Acad Sci U S A*. 2018;115:E8368–77.
- Zhu Z, Gan X, Fan H, Yu H. Mechanical stretch endows mesenchymal stem cells stronger angiogenic and anti-apoptotic capacities via NFκB activation. *Biochem Biophys Res Commun*. 2015;468:601–5.
- Chen X, Yan J, He F, Zhong D, Yang H, Pei M, et al. Mechanical stretch induces antioxidant responses and osteogenic differentiation in human mesenchymal

stem cells through activation of the AMPK-SIRT1 signaling pathway. *Free Radic Biol Med*. 2018;126:187–201.

- Melo E, Garreta E, Luque T, Cortiella J, Nichols J, Navajas D, et al. Effects of the decellularization method on the local stiffness of acellular lungs. *Tissue Eng Part C Methods*. 2014;20:412–22.
- Silva JD, Lopes-Pacheco M, Paz AHR, Cruz FF, Melo EB, de Oliveira MV, et al. Mesenchymal stem cells from bone marrow adipose tissue, and lung tissue differentially mitigate lung and distal organ damage in experimental acute respiratory distress syndrome. *Crit Care Med*. 2018;46:e132–40.
- Campillo N, Jorba I, Schaedel L, Casals B, Gozal D, Farré R, et al. A novel chip for cyclic stretch and intermittent hypoxia cell exposures mimicking obstructive sleep apnea. *Front Physiol*. 2016;7:319.
- Curley GF, Hayes M, Ansari B, Shaw G, Ryan A, Barry F, et al. Mesenchymal stem cells enhance recovery and repair following ventilator-induced lung injury in the rat. *Thorax*. 2012;67:496–501.
- Chimenti L, Luque T, Bonsignore MR, Ramírez J, Navajas D, Farré R. Pre-treatment with mesenchymal stem cells reduces ventilator-induced lung injury. *Eur Respir J*. 2012;40:939–48.

Paula N. Nonaka<sup>a,◇</sup> Bryan Falcones<sup>a,◇</sup> Ramon Farre<sup>a,b,c</sup>  
Antonio Artigas<sup>b,d</sup> Isaac Almendros<sup>a,b,c,\*</sup> Daniel Navajas<sup>a,b,e</sup>

<sup>a</sup> *Unitat Biofísica i Bioenginyeria, Facultat de Medicina i Ciències de la Salut, Universitat de Barcelona, Barcelona, Spain*

<sup>b</sup> *CIBER de Enfermedades Respiratorias, Madrid, Spain*

<sup>c</sup> *Institut d’Investigacions Biomèdiques August Pi Sunyer, Barcelona, Spain*

<sup>d</sup> *Critical Care Center, Corporació Sanitària i Universitària Parc Taulí, Institut d’Investigació i Innovació Parc Taulí, Sabadell, Spain*

<sup>e</sup> *Institute for Bioengineering of Catalonia, The Barcelona Institute of Science and Technology, Barcelona, Spain*

\* Corresponding author.

E-mail address: isaac.almendros@ub.edu (I. Almendros).

◇ Equally contributed to this work.

<https://doi.org/10.1016/j.arbres.2019.08.014>

0300-2896/ © 2019 Published by Elsevier España, S.L.U. on behalf of SEPAR.

## Anesthetic Management of Montgomery T-tube Insertion Via Rigid Bronchoscopy for Subglottic Complete Stenosis



### Manejo de la anestesia durante la inserción del tubo en t montgomery via broncoscopia rígida para el tratamiento de la estenosis subglótica completa

Dear Editor:

The Montgomery T-tube (hereinafter referred to as “T-tube”) is a treatment option for tracheal stenosis.<sup>1</sup> The indications for T-tube placement are typically temporary preoperative airway support, postoperative surgical reconstruction, or as an alternative method in case of surgical failure (restenosis or nonunion of anastomosis after surgery).<sup>2</sup> However, this approach has become an option for patients with benign airway stenosis who are unsuitable or unwilling to undergo surgery, as T-tube placement involves less trauma, is lower risk, is well-tolerated, and allows surgical intervention in cases of failure.<sup>3,4</sup> During T-tube insertion, the airway must be shared by a respiratory interventional physician and anesthesiologist, and the use of various modes of mechanical ventilation can complicate anesthetic management. There are few reports regarding anesthetic management during T-tube insertion in patients with complete tracheal stenosis (Myer-Cotton grade 4: occlusion).<sup>5</sup> We describe 5 cases of T-tube insertion via rigid bronchoscopy (RB) under general anesthesia with subglottic complete stenosis (Myer-Cotton grade 4) and discuss their anesthetic management.

All patients provided written informed consent and the use of clinical data was approved by the Institutional Review Boards of Beijing Tiantan Hospital affiliated to Capital Medical University (JS2013-007-02). **Table 1** shows the characteristics of the patients. All five patients refused to undergo surgery and chose T-tube placement (**Fig. 1**).

After intravenous administration of midazolam 0.03 mg/kg and sufentanil 0.1–0.2 µg/kg, the metal tracheotomy tube was replaced with a 7# disposable plastic cuffed tube connected to a Bain’s circuit and attached to a capnometer sampler. Anesthesia was induced with sufentanil 0.1–0.2 µg/kg, etomidate 0.3 mg/kg, and cisatracurium 0.2 mg/kg IV, maintained with propofol 4.5–6 mg/kg/h, remifentanyl 0.10–0.20 µg/kg/min, sufentanil and cisatracurium as required. BIS was maintained 40–60 during operation. After induction of anesthesia, an RB was placed. In cases 2–5, the guide wire passed through the stenosis via RB. Balloon dilators were inserted along the wire to the stenosis segment, and then dilatations were performed. In Case 1, the guide wire was unable to pass through the stenosis via RB because of occlusion. After removal of the tracheotomy tube, the jugular vein needle was passed retrograde from the tracheotomy hole through the stenosis toward the cephalad direction. The guide wire was then placed through the needle. During this process, if SPO<sub>2</sub> fell to 85%, the needle was removed and the tracheotomy tube was applied for ventilation until SPO<sub>2</sub> returned to 100%. After the guide wire could be observed via RB, the needle was removed; then, the balloon dilator, electro cauterizer, and forceps were inserted via RB along the wire to relieve stenosis. The balloon dilator (No. 5842, Boston Scientific, diame-